Advances in Science and Technology Research Journal

Advances in Science and Technology Research Journal, 2026, 20(3), 148–160
https://doi.org/10.12913/22998624/213902
ISSN 2299-8624, License CC-BY 4.0

Received: 2025.10.06
Accepted: 2025.12.03
Published: 2026.02.01

Effect of stirring speed, particle size, and Si_3N_4 content on the mechanical and corrosion properties of Al1050 matrix composites

Waleed Turki Rashid[1]

[1] College of Production and Metallurgy Engineering, University Technology, Baghdad, Iraq
E-mail: waleed.t.rashid@uotechnology.edu.iq

ABSTRACT

This study investigated how stirring speed, particle size, and Si_3N_4 content affect the strength, hardening, and corrosion properties of Al1050, using MINITAB 16 software to analyze the results. The composite material was made by mixing different amounts of Si_3N_4 (2, 4, and 6 wt%), using Si_3N_4 particles of sizes 32, 44, and 53 micrometers, and stirring at different speeds of 300, 600, and 900 revolutions per minute. The stir casting technology was employed to manufacture a composite material. The microscopic structure was analyzed utilizing SEM microscopy. The results for the best tensile strength and hardening values of 202 MPa and 66 kg/mm² were reached with the settings of X1 = 900 rpm, X2 = 44 µm, and X3 = 6 wt%. The optimum tensile strength was determined to be 212.55 MPa, achieved with parameters X1 = 900 rpm, X2 = 32 µm, and X3 = 6 wt%, as indicated by the program. This result closely aligns with the practical test outcome, which recorded a tensile strength of 209.7 MPa, demonstrating a strong correlation with the findings from the program. Both tensile strength and hardness improve with increasing stirring speed and reinforcing percentage, indicating their substantial influence. As particle size increases, tensile strength and hardness first fall and then slightly rise. The stirring speed has the most significant impact, whereas the particle size has the least influence on the mechanical properties. Regarding the chemical characteristics, corrosion tests measuring weight loss have been conducted on MMC and related base alloys utilizing exposure durations (5–30 min), temperatures (25 °C), as well as corrosive fluids of 3.5% NaCl, where the composites are less prone than the matrix to corrosion and pitting. It was discovered that the weight loss of base alloys and MMC increased with contact time. Additionally, it was discovered that both the base alloy and the composite materials corrode more when the temperature rises. It was observed that the corrosion rate decreased with increasing Si_3N_4 reinforcement.

Keywords: AL-1050 alloy, composite materials, weight loss method, stir casting process, MINITAB statistical analysis.

INTRODUCTION

Metal matrix composites (MMCs) are gaining popularity because of their unique mechanical properties, such as their high elastic modulus and low weight. Aluminum applications are limited when both high modulus and higher strength are required because it is a rather weak and lightweight metal. Despite the development of high-strength aluminum alloys, the enhancement of alloy stiffness has not been significantly impacted by the addition of alloying elements or microstructural control. MMCs are an advancement in materials that are lightweight, high modulus, and high strength [1]. The primary advantage of aluminum lies in its versatility as a reinforcement material in aluminum matrix composites [2]. Materials with improved mechanical qualities and resilience to high temperatures, including composites, are currently in substantial demand across numerous industries. Materials known as composites are created when two or more components in different chemical and physical phases are combined. In real-world applications, metal matrix composites are used to create the materials with improved mechanical qualities, such as high tensile strength, hardness, and toughness [3]. These materials are

used in various aerospace applications, including braking drums, discs, cylinder liners, jet engine vanes, helicopter blade sleeves, and components of the space shuttle [4]. The optimal method for manufacturing liquid-state metal composite materials is stir casting [5]. The most straightforward and popular method is the vortex technique, also referred to as the stir-casting technique. This method creates a vortex at the melt surface by melting the matrix material and then vigorously stirring it. Then, from the vortex side, the reinforcing material is added. Composites are synthesized by stir casting [6]. Metals and their alloys, ceramics, and polymers are the main categories of matrix materials. Composites are categorized as ceramic matrix composites, metal matrix composites, and polymer matrix composites based on these classifications. An aluminum phase plus an extra reinforcing element, which could be metallic or non-metallic (such as ceramic or organic material), make up an aluminum matrix composite. Metal matrix composites are made by adding reinforcing materials to the aluminum matrix, which improves the strength, wear resistance, and overall properties of the final product [7]. Aluminum exhibits certain characteristics including availability, low density, malleability, superior electrical conductivity, advantageous thermal properties, energy efficiency, and environmental sustainability, making it superior to other metal matrix composites. Aluminum matrix composites can withstand high temperatures, radiation, and moisture, and they also have great strength as well as electrical and thermal conductivities [8]. Typically, carbides exhibit superior wetting and bonding properties relative to nitrides. The incorporation of Si_3N_4 particles into the matrix is expected to improve the wettability within AMCs. Historical literature indicates that Si_3N_4 ceramic particles exhibit a greater contact angle with molten aluminum, resulting in diminished wettability properties [9,10].

Shalaby et al. [11] proposed that reinforcing Si_3N_4 ceramic particles with an aluminum alloy composite can be effectively carried out using the stir casting method. Because gases are added while melting, the stir casting process significantly lowers porosity, increasing the densities of composites. The Al-Si_3N_4 composite made by Rao et al. [12] using the stir casting process had improved ultimate tensile strength and hardness. Using the stir casting method, Kumar et al. [13] created A7075-silicon nitride composites, which showed improvements in density and decreased porosity. Imtiaj et al. [14] studied the impact of incorporating aluminum oxide (Al_2O_3) and titanium dioxide (TiO_2) into an aluminum matrix to develop composite materials characterized by a high strength-to-weight ratio. High-purity aluminum powder (99.9%) was utilized, combined with varying ratios of Al_2O_3 and TiO_2 (2.5%, 5%, 7.5%) by the stir casting technique. The results showed that adding Al_2O_3 and TiO_2 made the material less dense, but the strongest sample was the one with 5% of each, which also had better impact strength. This composite is deemed appropriate for the engineering applications necessitating a high strength-to-weight ratio. Ahmed et al. [15] studied the investigation of the impact of incorporating Al_2O_3 and carbon (C) on the characteristics of an aluminum matrix. The matrix was fabricated using stir casting with equal ratios of Al_2O_3 and carbon (2.5%, 5%, 7.5%, and 10% by weight). Analyses were conducted on the phase, microstructure, density, hardness, impact strength, and tensile strength. The interaction between the matrix and the reinforcing elements resulted in the appearance of a new phase, according to X-ray diffraction (XRD) research. Images from scanning electron microscopy (SEM) showed that the particles were evenly distributed throughout the matrix. A reduction in density and hardness was noted alongside an increase in carbon content, although impact strength improved. The hybrid matrix of 5% Al_2O_3 and 5% carbon demonstrated the highest tensile strength. These hybrid composites are advantageous in applications like the production of standard bolts. Shrishail et al. [16] studies were conducted to create metal matrix composites using Al7020 alloy mixed with fine boron carbide (B_4C) particles through the stir casting method. The findings indicated that incorporating up to 8% B_4C enhanced tensile strength, hardness, and compressive strength, although it resulted in a minor reduction in elongation, thereby illustrating the effectiveness of reinforcement in improving mechanical properties.

The objective of this study is to produce an metal matrix composite (MMCs) made from Al1050 reinforced with Si_3N_4, and then evaluate the mechanical and chemical properties of base alloy (unreinforced) aluminum 1050 and composites by testing on factors according to various levels using software Minitab.

EXPERIMENTAL WORK

Materials used

Aluminum alloy 1050 is recognized for its corrosion resistance, elevated ductility, and highly reflective polish, containing additional chemical components in quantities less than 0.4% alongside the primary aluminum metal. Alloy Al-1050 was utilized as a matrix for the fabrication of composite materials reinforced with Si_3N_4. The analysis of Al-1050 cast alloy was conducted using Spectro Max by the State Company for Inspection and Engineering Rehabilitation, as presented in Table 1.

Preparation of composite materials

A composite material was prepared using the stir casting method with a vortex technique. The base alloy was melted in an electric furnace equipped with a top slot, utilizing a graphite crucible at a temperature of 750 °C. Once the material has completely melted, Si_3N_4 reinforcing material was introduced, characterized by a particle size distribution of (+33 -50 µm). The matrix alloy was initially superheated beyond its melting temperature to generate a vortex in the melt, utilizing a stainless-steel mechanical stirrer. The impeller depth is roughly one-third of the height of the melt measured from the bottom of the crucible. Si_3N_4 particles were encased in aluminum foil and preheated to 300°C. Subsequently, the particles were gradually introduced into the melt, and stirring was maintained for approximately five minutes at an average speed of 500 rpm. The molten metal was introduced into a preheated cast iron mold at 250 °C, featuring dimensions of 15 mm in diameter and 100 mm in height. Figure 1 illustrates the stir casting method.

Tensile test

All specimens produced in this investigation underwent a tensile test in compliance with ASTM E-8 criteria [11]. As it was shown in Figure 2, the test samples were formed into a cylindrical specimen with a 7 mm diameter and a 36 mm gauge length. Using an Instron universal testing instrument, the investigation was performed at room temperature with an extension rate of 1 mm/min. The stress-strain curves produced during the tension tests were used to measure the tensile parameters, which included elongation, yield strength, and ultimate tensile strength. The sample post-casting is shown next to the specimens in Figure 3, both before and after tensile testing.

Table 1. Chemical composition [%] of aluminum alloy 1050

Si	Fe	Cu	Mn	Zn	Ti	Mg	Al
0.25	0.4	0.05	0.05	0.07	0.05	0.05	Remainder

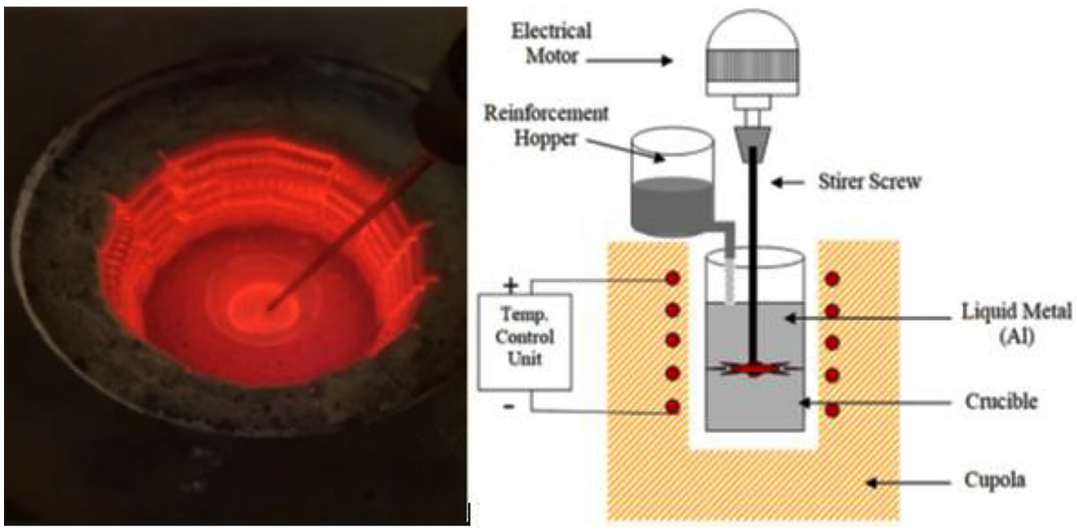

Figure 1. Stir casting technique

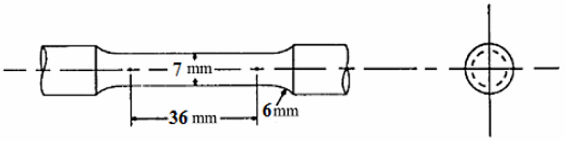

Figure 2. ASTM standard tensile specimen

Figure 3. The sample after casting and the samples before and after tensile testing

Hardness test

The base alloy and composite material samples were subjected to a load of 0.8 kg for 15 seconds to determine their hardness using a Hensoldt Wetzlar No. 2398 Vickers hardness tester. At least three hardness readings are obtained from various points for every specimen. Equation 1 was used to compute Vickers hardness [18].

$$VH = 1.8544 \times P/d(av)^2 \quad (1)$$

where: VH – Vickers macro hardness (kg/mm^2), $d(av)^2$ – average indentation diameter (mm), P – applied load (kg).

Corrosion test

By immersing the specimens in a 3.5 percent NaCl solution, the weight loss technique was used to assess the test data as well as analyze the corrosion parameters of the matrix alloy and the metal matrix composite (MMC). The test specimens were trimmed to dimensions of 25 mm by 12 mm before being ground using emery paper ranging from grades 220 to 1000 to achieve a polished finish. The samples have subsequently been degreased using acetone. Following rinsing in distilled water, the specimens were air-dried and subsequently immersed in 3.5 wt% NaCl solutions at 25 °C. The weight reduction measurements pertained to a duration of 5–30 min. Figure 4 illustrates the corrosion samples prior to and following the test.

$$(\Delta W = W2 - W1) \quad (2)$$

where: ΔW – weight loss average,
$W2$ – final weight, $W1$ – initial weight.

DESIGN OF EXPERIMENTS

Designing experiments involves a series of steps to collect the necessary data and organize it in a table suitable for statistical analysis, which facilitates the drawing of useful conclusions for real-world applications [19]. The process factors substantially affect the tensile strength and hardness of the components. Table 2 delineates the separate controllable process parameters that significantly influence tensile strength and hardness. The goal of varying tensile strength and hardness is to investigate how specific factors, stirring speed (X1), particle size (X2), and Si_3N_4 percentage (X3), affect them to determine the optimal values for achieving the highest tensile strength and hardness. Table 2 enumerates all the criteria examined in the current investigation. Table 3 presents the experimental results alongside the experimental methodology (Matrix). Minitab 16 was employed to statistically analyze the cumulative impacts of process factors on tensile strength and hardness. All coefficients were evaluated for significance within a 95% confidence interval.

Figure 4. Corrosion samples before and after test 4%wt

Table 2. Parameters and their levels

Parameters	Codes	Notations	Unit	Levels		
				-1	0	+1
Stirring speed	S.S	X1	rpm	300	600	900
Particle size	P.S	X2	μm	32	44	53
Si_3N_4 percentage	T.P	X3	wt%	2	4	6

Table 3. Matrix of experimental design and recorded wear rate values

No	X1	X2	X3	S. S	P. S	T. P	Tensile strength (MPa)	Hardness (kg/mm) ^{2}
1	-1	-1	0	300	32	4	111	32
2	1	-1	0	900	32	4	200	64.6
3	-1	1	0	300	53	4	109	28
4	1	1	0	900	53	4	198	62.8
5	-1	0	-1	300	44	2	98	27.2
6	1	0	-1	900	44	2	120	37
7	-1	0	1	300	44	6	136	39
8	1	0	1	900	44	6	202	66
9	0	-1	-1	600	32	2	161	45
10	0	1	-1	600	53	2	148	41.4
11	0	-1	1	600	32	6	183	58
12	0	1	1	600	53	6	180	55
13	0	0	0	600	44	4	171	52.2
14	0	0	0	600	44	4	168	49.5
15	0	0	0	600	44	4	168	48.2

RESULTS AND DISCUSSION

Microstructural study

Microstructural examination of the produced samples was conducted using SEM. Figures 5A and 5B depict SEM images of pure Al1050 alloy and Si_3N_4-reinforced composites. Figure 5A displays the scanning electron microscope (SEM) image of a pure Al1050 alloy. Figure 5B displays the micrographs of Al1050 composites with 6 wt.% Si_3N_4. The micrograph indicates that the reinforcement particles are uniformly dispersed within the aluminum matrix. The importance of this equitable distribution cannot be overstated. The primary advantage is the enhanced mechanical properties of the composite due to optimized load transfer between the matrix and the reinforcing particles. This equitable distribution also reduces the formation of particle clusters or agglomerates, which could otherwise lead to stress concentration and potential failure spots. To attain enhanced mechanical properties, such as increased strength and hardness, a uniform dispersion of particles inside the composite is required, as it contributes to greater hardness. Furthermore, the dispersion of Si_3N_4 particles augments the rigidity and tensile strength of the composite.

Test of significance

The linear regression model was employed in MINITAB 16, as indicated by the experimental results in Table 4. The regression equations are shown in equations 3 and 4.

$$Y = 125.5 + 0.349X1 + 0.054X2 + 8.875X3 + 0.022X11 + 0.064X22 + 2.063X33 + 0.021X12 + 0.018X13 + 0.173X23 \quad (3)$$

A p-value of 0.05 is considered significant, while the values exceeding this threshold are deemed insignificant and can be disregarded. The regression equation can be reformulated as follows:

$$Y = 125.5 + 0.349X1 + 0.054X2 + 8.875X3 + 0.022X11 + 0.018X33 + 2.063X13 \quad (4)$$

The variables X1, X2, and X3 denote stirring speed, particle size, and the percentage of Si_3N_4 particles, respectively, while Y represents tensile

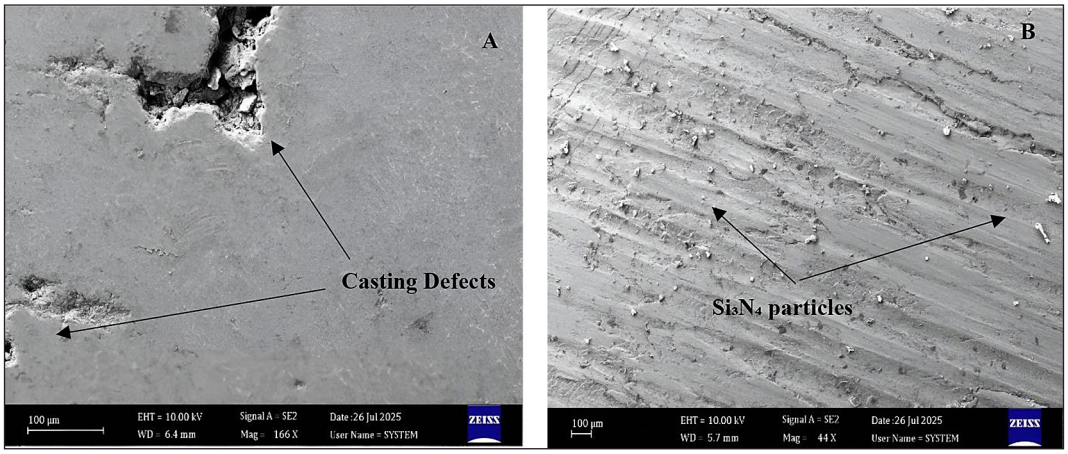

Figure 5. SEM images of (A) Al050 alloy, (B) Al1050-6% Si_3N_4 composites

Table 4. Response surface regression: Y versus X1, X2 and X3

Regression coefficients	Term	Coefficients value	SE coefficient	T-value	P-value
b0	Constant	125.5	193.6	0.648	0.000
b1	S. S	0.349	1.920	1.920	0.003
b2	P. S	0.054	0.800	-0.800	0.001
b3	T. P	8.875	0.325	0.325	0.000
b11	S.S*S. S	0.022	-2.380	-2.380	0.008
b22	P.S*P. S	0.064	0.751	0.751	0.063
b33	T.P*TP	0.018	-0.903	-0.903	0.007
b12	S.S*P. S	0.021	-0.182	-0.182	0.063
b13	S.S*T. P	2.063	1.253	1.253	0.002
b23	P.S*T. P	0.173	0.417	0.417	0.094

strength. Equation 4 indicates that stirring speed (X1) significantly influences tensile strength, whereas the effects of particle size (X2) and Si_3N_4 particle percentage (X3) are comparatively minor. The Si_3N_4 percentage (X3) exhibited a more significant effect than the particle size (X2). Alongside the individual effects of the variables, a collective influence on tensile strength was also noted.

Analysis of variance (ANOVA)

The important design parameters affecting hardness and tensile strength were identified using the ANOVA test. With a significance threshold of 0.05 and the regression model's F-test, Table 5 shows that the P-value is less than 5%, indicating the significance of the regression model; this is a desirable outcome [20]. The independent variables (X1, X2, and X3) are responsible for 84.61% of the changes in the dependent variable (Y), with the remaining portion being attributed to other factors, such as random error, according to the adjusted R-squared of 84.61%.A coefficient of determination approaching one indicates optimal performance and can yield exceptional results.

Normal probability plot

A graphical tool for assessing the approximate normality of the data set is the normal probability plot. Plotting the data against a hypothetical normal distribution should result in points that roughly resemble a straight line. Deviations from this linear trajectory signify deviations from normalcy. Normal probability plots were produced using the MINITAB16 program. Figure 6 illustrates that all data residuals have an almost normal distribution since the overall points form a nearly straight line.

The main effect plot of tensile strength

Stirring speed, particle size, and Si_3N_4% all have distinct effects on the tensile strength for values between 1 and -1, as seen in Figure 7. The

Table 5. Analysis of variance for Y

Source	DF	Seq SS	Adj MS	F-value	P-value
Regression	9	15463.5	15463.5	5.57	0.002
Residual error	5	1542.2	1542.2		
Total	14	17005.7			
R-Sq = 90.93%		R-Sq(adj) = 84.61%		S = 1.75	

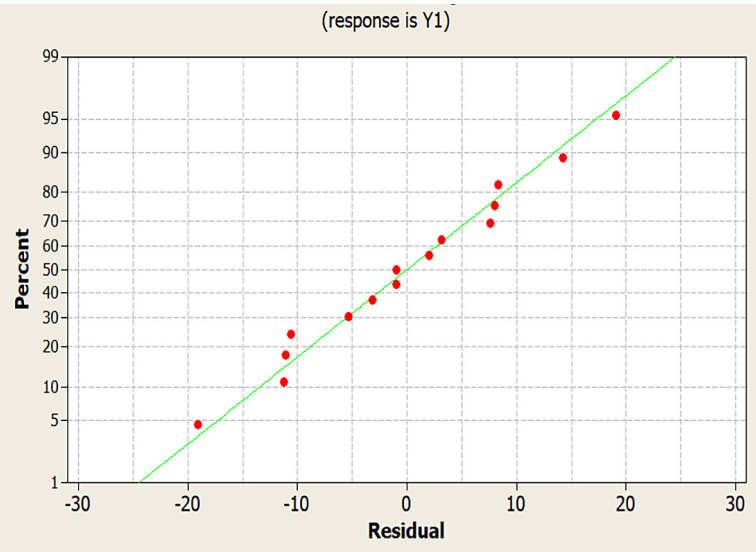

Figure 6. Normal probability plot of residuals of tensile strength

tensile strength gradually increases as the stirring speed and Si_3N_4 concentration are increased. This trend is attributed to the effective dispersion of Si_3N_4 particles within the matrix alloy as the stirring speed increases, particularly in terms of the proportion of Si_3N_4 particles. Increasing the Si_3N_4 percentage is expected to improve how well the particles spread out in the Al-1050 matrix, which will make the structure stronger; this result agrees with [21]. The temperature differential between the ceramic particles and the aluminum matrix is most likely what caused the strength rise, which is a key way to raise the number of dislocations in the matrix. Consequently, these changes will directly enhance the strength of the MMC, thereby increasing the resistance to plastic deformation, which subsequently results in elevated tensile strength, a phenomenon also shown in [22, 23].

Augmenting the particle size of Si_3N_4 results in a reduction of tensile strength until reaching a size of 44 μm, after which tensile strength begins to marginally increase with further enlargement to 53 μm. This happens because larger particles are more likely to separate from the mixture, which causes them to settle in the alloy and, as a result, lowers the tensile strength, a conclusion supported by the study [24]. It is well known that composites with smaller particles have better surface energy between the reinforcement and the matrix, and the particles are closer together. This helps transfer force from the softer matrix to the harder reinforcement, which improves the composite strength and ability to harden under stress. The experimental results show that making the reinforced particles smaller leads to closer spacing between them and higher work-hardening rates, which can improve the structure and strength of the composite for a specific number of particles used. Enhancements in strengthening are observed as particle size diminishes. As the size of the Si_3N_4 particles becomes smaller, the area where the matrix and the Si_3N_4 particles touch increases, making it easier for more force to transfer from the matrix to the Si_3N_4 particles. A larger surface area between the materials can help the matrices create more changes, tiny cracks, gaps, and breaks, which can enhance their strength. Heavier particles, conversely, collapse more swiftly than smaller particles during the tensile-testing procedure for two significant

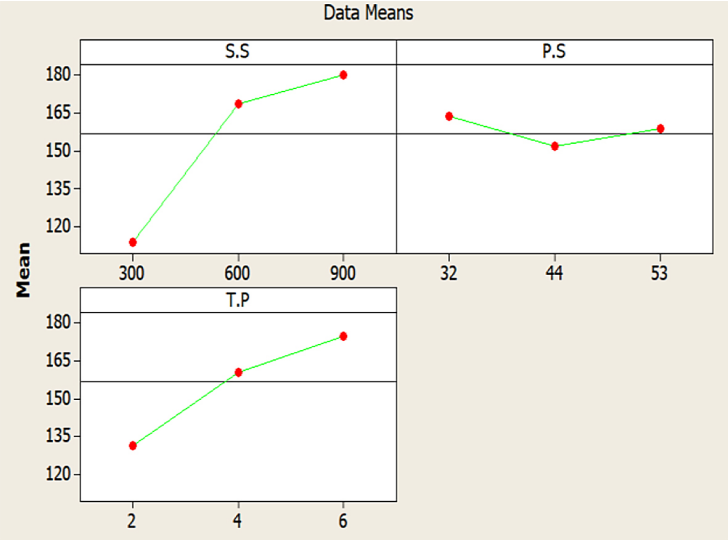

Figure 7. Main effect plot to tensile strength

reasons [25]. Larger particles possess a greater interaction area with the matrix, resulting in heightened stress concentration. Furthermore, the inherent flaws within the particle affect its fracture toughness. Because larger particles have a size limit on faults, they are more likely to break, as they have a much higher chance of developing a flaw or imperfection that exceeds the critical size. This results in reduced tensile strength because the fragmented particles cannot withstand stress and serve as preferred sites for failure. Numerous researchers have corroborated that incorporating filler into the composite enhances its tensile properties. The better tensile properties are due to the high quality of the particles, strong bonding between the reinforcements and the matrix, as well as low levels of empty spaces [26, 27].

Response surface analysis

Figures 8A, C, and E present three-dimensional plots, while Figures 8B, D, and F display contour plots that illustrate how components (X1, X2, and X3) affect response Y. A three-dimensional contour figure illustrates the effect of stirring speed, particle size, and weight percentage of SiN_4 particles on tensile strength. The tensile strength increases as the weight fraction and stirring speed increase. Conversely, it was shown that tensile strength diminishes and then experiences a minor increase along with particle size. Nonetheless, it was noted that the synergistic influence of stirring speed and the Si_3N_4 proportion is more pronounced.

Optimization of tensile strength

Figure 9 illustrates the optimization chart for tensile strength across varying levels of three parameters (X1, X2, and X3). The result optimizations are displayed in the left column, whereas the optimal settings for each parameter are presented in the center of the top row. The behavioral curve of each element is illustrated below. According to the table, a tensile strength of 212.55 MPa can be obtained under ideal conditions of stirring speed (900 rpm), SiN_4 particle size (32 µm), and weight fraction (6 wt%). When the values for string speed (X1), particle size (X2), and Si_3N_4 (X3) calculated using the program were used in real-world applications, the resulting tensile strength of 209.7 MPa nearly matched the program output.

Hardness test

Figure 10 illustrates the Vickers hardness values (HV) corresponding to different stirring speeds, particle sizes, and Si_3N_4 percentages (X1, X2, and X3), respectively. The tensile strength and hardness tests demonstrated notable similarities in behavior when the weight percentage of Si_3N_4 particles and stirring speed varied with an increase in particle size. The optimal hardness value of 66 kg/mm² was observed in sample number 8 (X1=900 rpm, X2=44 µm, X3=6 wt%), while the minimal hardness value of 27.7 kg/mm² was recorded in sample number 5 (X1=300 rpm, X2=44 µm, X3=2 wt%). Improvement in hardness and tensile strength with the addition of ceramic particles this result agrees with [28, 29].

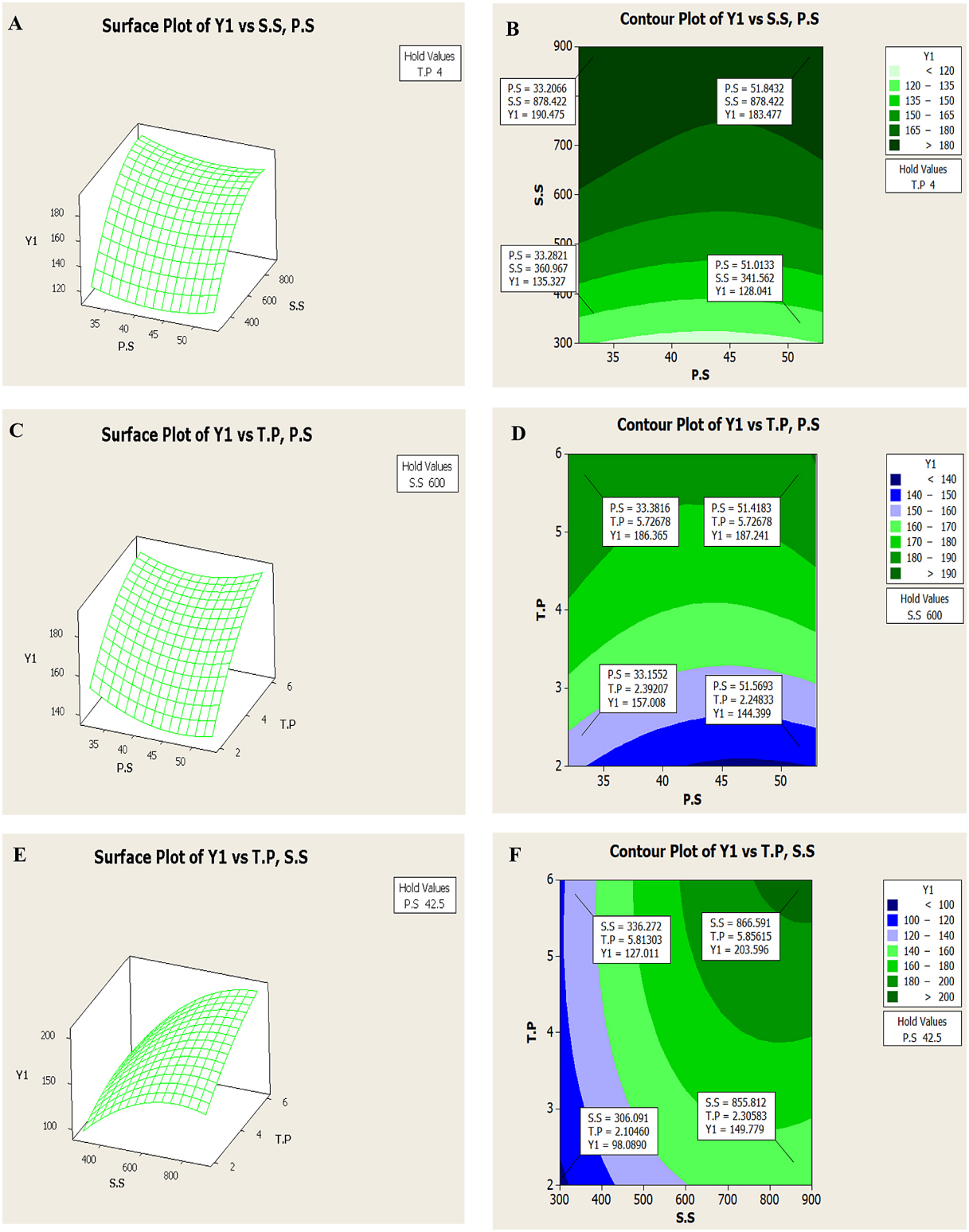

Figure 8. Three-dimensional and Contour plot of tensile strength, effects of variables X3 and X2 on a response (Y)

Weight loss corrosion test

Figure 11 illustrates the Al-1050 matrix and composite material, demonstrating the correlation between weight loss and exposure time. The corrosion measurement in the static immersion test is a function of exposure time, and all alloys exhibit an increase in corrosion as the test duration increases. The graph shows that as exposure duration grows, so does the composite resistance to corrosion. This method eliminates the chance of hydrogen bubbles adhering to the specimen

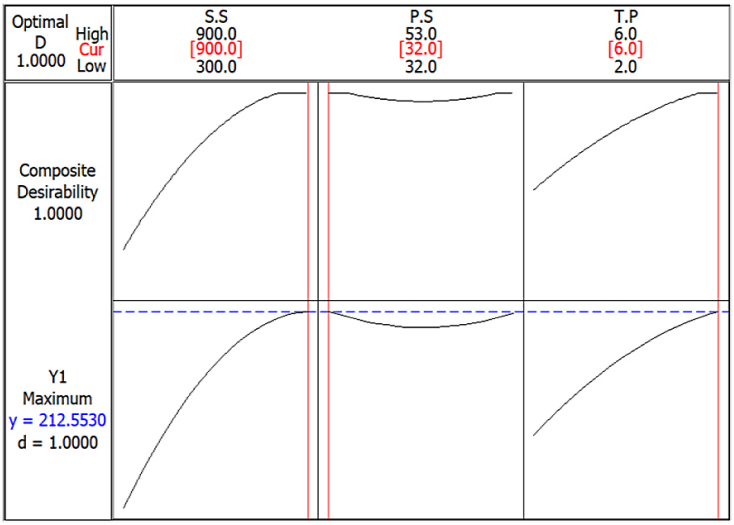

Figure 9. Optimization chart for maximum tensile strength

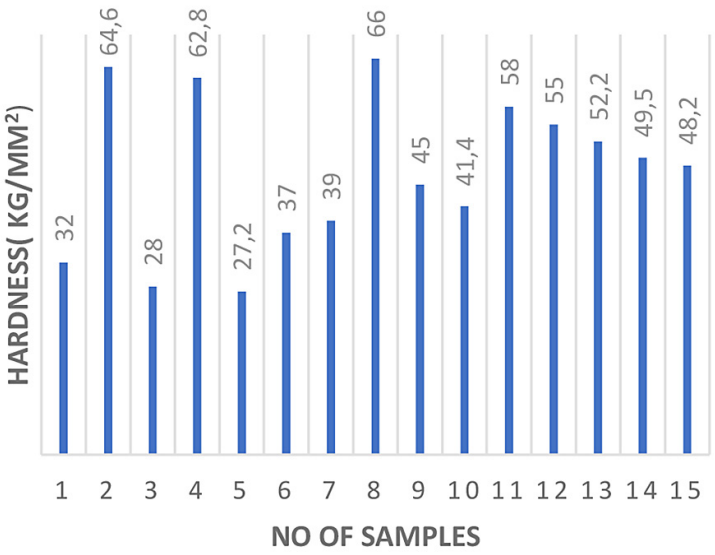

Figure.10 Hardness test of alloy and composite

surface and creating a long-lasting coating that interferes with the corrosion process. In contrast to composite materials, the Al-1050 alloy exhibits a substantial weight loss. Due to the absence of any reinforcement, the base alloy is incapable of offering any form of resistance to the medium. Therefore, the weight reduction in the case of an unreinforced alloy is greater than that of composites; this result agrees with [30, 31]. This assumption is logical, as the area of the aluminum matrix exposed to the corrosive solution will decrease due to the added materials [32].

Figure 12, which shows the SEM image of the aluminum alloy reinforced with 4% wt Si_3N_4 after exposure to a 3.5% NaCl solution, reveals the surface topography that indicates the onset of corrosion effects. The carbide particles are distributed within the aluminum matrix, with signs of possible galvanic corrosion between the metallic matrix and the ceramic reinforcement, as suggested by localized contrast variations. No deep pitting corrosion is observed, suggesting an initially satisfactory resistance to the chloride environment, although further degradation may occur over time.

Figure 13 shows the specimens that underwent corrosion testing at elevated temperatures ranging from 25 °C to 55 °C for a fixed duration of 30 minutes. The findings demonstrated that the corrosion rate escalated with temperature across all alloys. The acceleration of electrochemical reactions at

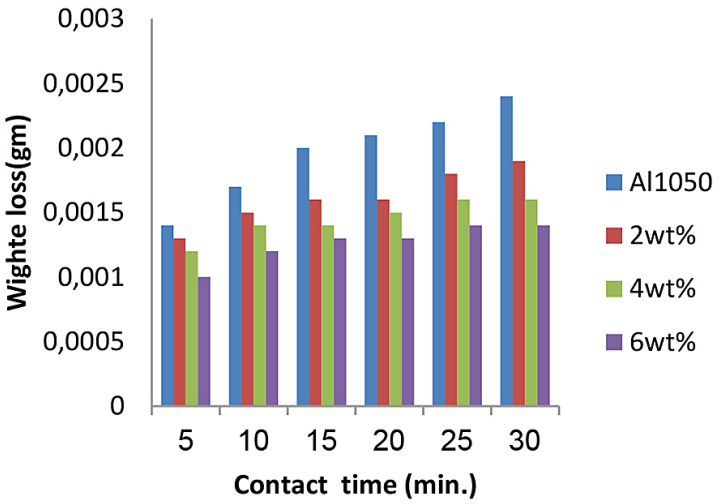

Figure 11. Weight loss Vs exposure time of Al-1050 alloy and composite materials

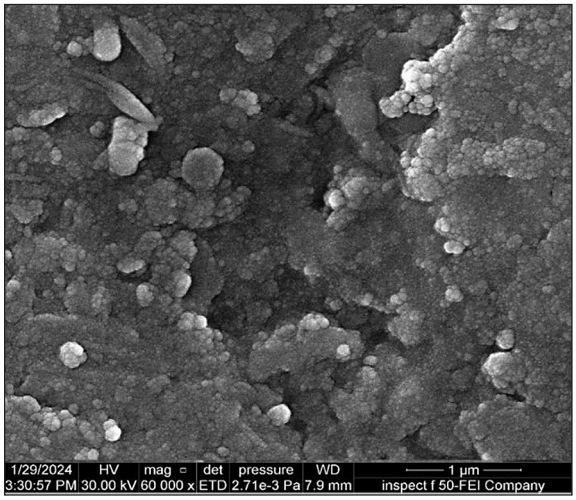

Figure 12. SEM image of the aluminum alloy reinforced with 4% wt Si_3N_4 after exposure to a 3.5% NaCl solution

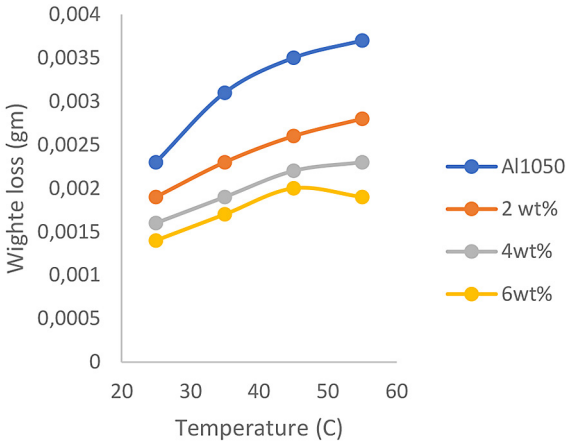

Figure 13. Working temperature Vs corrosion rate in 3.5 NaCl for 30 minutes of exposure

elevated temperatures is attributed to increased thermal energy, which enhances ion mobility and reaction kinetics on the metal surface, often resulting in the degradation of passive protective layers [33, 34]. The severity of corrosion differed among the alloys. The unreinforced Al1050 alloy exhibited the greatest weight loss, signifying its reduced resistance to corrosion under thermal stress. The incorporation of Si_3N_4 markedly enhanced corrosion resistance, and increased Si_3N_4 content was associated with reduced weight loss. The enhancement is primarily attributed to the inert and robust characteristics of Si_3N_4 particles, which strengthen the microstructure and reduce the surface reactivity of the alloy. Si_3N_4 enhances the formation of a more chemically stable surface barrier [35]. The alloy containing 6% Si_3N_4 demonstrated superior performance, validating the efficacy of metal matrix composites in improving corrosion resistance, particularly in thermally fluctuating environments.

CONCLUSIONS

On the basis of the research results obtained in this work, the following conclusions were presented:

1. The incorporation of Si_3N_4 into the Al-1050 alloy enhanced its tensile strength, hardness, and corrosion resistance.
2. Regression models can be written as Y = 125.5 + 0.349X1 + 0.054X2 + 8.875X3 + 0.0022X11 + 0.018X33 + 2.063X13, showing that X1 and

X3 have a great impact on tensile strength and hardness, while X2 has a smaller effect compared to X1 and X3.

3. The increase in the weight fraction (X3) and stirring speed (X1), along with the decrease in the Si_3N_4 particles (X2), results in enhanced tensile strength and hardening value.
4. The optimal tensile strength and hardening achieved were 212.55 MPa and 66 kg/mm², respectively, with a stirring speed of 900 rpm, a Si_3N_4 particle size of 32 µm, and a weight fraction of 6 wt%.
5. Corrosion resistance is increased when SiN_4 is added to Al-1050 alloy; however, it is decreased with extended contact time. The particles were evenly distributed throughout the matrix system, according to the microstructure analysis. Furthermore, it was shown that when the temperature rises, corrosion increases for both the base alloy and the composite materials. As Si_3N_4 reinforcement increased, the corrosion rate was found to decrease.

REFERENCES

1. Wagih A., and Fathy A. Experimental investigation and FE simulation of nano-indentation on Al–Al_2O_3 nanocomposites. Adv Powder Technol. 2016; 27(22): 403–410. https://doi.org/10.1016/j.apt.2016.01.021
2. Fathy A., Omyma E., Mohammed M. Effect of iron addition on microstructure, mechanical and magnetic properties of Al–matrix composite produced by powder metallurgy route. Trans Nonferrous Metals Soc China.2015; 25: 46–53. https://doi.org/10.1016/S1003-6326(15)63577-4
3. Kumar B., Gopalarama G., Pragadish N.,Venkatesh P., Sanjay C., Navaneethakrishnan G., Suresh V., Venkatesan G. Investigations on Wear Behavior of Aluminium Composites at Elevated Temperature. Hindawi,Advances in Materials Science and Engineering; 2022(2022): 1–7. https//.doi:org/ 10.1155 /2022 /9594798.
4. Waleed R. and Khalid R. Improvement and optimization of the hardness for the aluminum metal matrix composite using eggshell. Materials Science Forum. 2021; 1039: 42–50. https://doi.org/10.4028/www.scientific.net/MSF.1039.42
5. Aherwar A., Patnaik A., Pruncu C. Effect of B4C and waste porcelain ceramic particulate reinforcements on mechanical and tribological characteristics of high strength AA7075 based hybrid composite. J. Mater. Res. Technol. 2022; 9(5): 9882–9894. https://doi.org/10.1016/j.jmrt.2020.07.003
6. Kumar A., Bhandari R., Aherwar A., Rimasauskiene R. Matrix materials used in composites: A comprehensive study. Mater. Today Proc.2020; 21(30): 1559–1562. https://doi.org/10.1016/j.matpr.2019.11.086
7. Hossain M., Ahmed M., Hassan T. An experimental study on mechanical properties of stir casted hybrid al metal matrix composite reinforced with Al_2O_3 and TiO_2. Journal of Engineering Advancements.2025; 6(1): 1–10. https: //doi. org/10. 38032/ jea.2025.01.001
8. Shekhawat D., Singh A., Banerjee M.K., Singh T., Patnaik A. Bioceramic composites for orthopaedic applications: A comprehensive review of mechanical, biological, and microstructural properties. Ceramics international.2021; 47(3): 3013–3030. https:// doi.org/ 10.1016 /j.ceram int.2020.09.214
9. Hasan L.M., Ali A.M., Naveen S. Assessment of eggshell and $CaCO_3$ reinf orced recycled aluminium green metal matrixI. Journal of Achievements in Materials and Manufacturing Engineering.2023; 118(2): 57–61. https://doi. 10.5604/01.3001.0053.7662
10. Aherwar A., Patnaik A., Pruncu C. Effect of B4C and waste porcelain ceramic particulate reinforcements on mechanical and tribological characteristics of high strength AA7075 based hybrid composite,» J. Mater. Res. Technol, 2020; 9(5): 9882–9894.
11. Shalaby E.A., Churyumov A.Y., Solonin A.N., Lotfy A.Preparation and characterization of hybrid A359/(SiC+ Si3N4) composites synthesized by stir/ squeeze casting techniques. Mater. Sci. Eng. 2016; 674:18–24. https://doi.org/10.1016/j.msea.2016.07.05
12. Kumar S.A., Vignesh J.H., Joshua S.P. Investigating the effect of porosity on aluminum 7075 alloy reinforced with silicon nitride (Si_3N_4) metal matrix composites through STIR casting process. Mater. Today Proc.2021; 39(1): 414–419. https: //doi.org/10. 1016/ j.matpr.2020.07.690
13. Shuaihang P. Tianqi Z. a, J Yuan., Kaiyuan J., Xiaochun L. TiB2 nanoparticles-regulated oxidation behavior in aluminum alloy 7075. Corrosion Science.2021; 191: 1–21. https: //doi.org /10.101 6/j.corsci.202 1.109749.
14. Nayim S., Hasan M., Seth P., Gupta P., Thakur S., Kumar D., Jamwal A. Effect of CNT and TiC hybrid reinforcement on the micro-mechano-tribo behaviour of aluminium matrix composites. Materials Today: Proceedings.2020; 21: 1421–1424. https://doi.org/10.1016/j.matpr.2019.08.203
15. Ahamad N., Mohammad A., Sadasivuni K., Gupta P.Phase microstructure and tensile strength of Al-Al_2O_3 hybrid metal matrix composites. Proceedings of the Institution of Mechanical Engineers. Part C: Journal of Mechanical Engineering Science. 2020; 234(13): 2681–2693. https://doi.org/10.1177/0954406220909846

16. Angadi S., Kumar S., Nagaral M., Auardi V., Valukula B. Effect of ceramic boron carbide particles addition on the mechanical and microstructural characteristics of Al7020 alloy composites. Mechanics of Advanced Composite Structures.2025; 12(24): 169–180. https: // cr eativ ecommo ns.org / licenses/by/4.0/
17. ASTM E 8M: Standard Test Method for Tension Testing of Metallic Materials (Metric), Annual Book of ASTM Standards, Philadelphia, (1991).
18. Waleed R., Optimization of wear resistance of aluminum matrix composite (Al 7050/10wt% eggshell) by study of effect stirring speed and stirring time. kufa journal of engineering.2025; 15(4): 83–97. https://doi.org/10.30572/2018/KJE/150407
19. Khalida M., Alaa S., Emad H., Tahseen A., Aqeel B.A. Statistical investigation and prediction of the effect of fdm variables on flexural stress of pla prints.Tikrit Journal of Engineering Sciences. 2024; 31(3): 10–17. https://doi.org/10.25130/tjes.31.3.2
20. Venkatprasat S., Subramaian R., Radhika N., Anandavel B., Arun L., Praveen N.Influence of parameters on the dry sliding wear behavior of aluminum\flyash graphite hybrid metal matrix composites. European Journal of Scientific Research. 2011; 53(2): 280–290.
21. Pankaj P. A., Shivprakash B. B. Microstructural observation and mechanical properties behavior of Al_2O_3/Al6061 nanocomposite fabricated by stir casting process. Engineering Research Express.
22. Nagaral M., Bharath V., Auradi V. Effect of Al2O3 particles on mechanical and wear properties of6061al alloy metal matrix composites. Material Science & Engineering 2013; 2(1): 1–4. https://doi:10.4172/2169-0022.1000120
23. Waleed R. Effect of Mg percentage and weight fraction of yttrium oxideon the tensile strength of aluminum matrix composite (Al-6061 /Y_2O_3). AIP Conf. Proc. 3002, 080026, 2024. https://doi.org/10.1063/5.0205902
24. Parvin N. and Rahimian M.The characteristics of alumina particles reinforced pure Al matrix composite proceedings of the international congress on advances in applied physics and materials science. Antalya, Turkey, 2012; 121(1): 108–110.https:// doi: 10.12693/APhysPolA.121.108
25. Sharma S., et al. Investigation on mechanical, tribological and microstructural properties of Al–Mg–Si–T6/SiC/muscovite-hybrid metal-matrix composites for high strength applications. J. Mater. Res. Technol. 2021; 12: 1564–1581. https://doi.org/10.1016/j.jmrt.2021.03.095
26. Rashmi P., Mahesh T., Zeeshan A., Veeresha G., Nagaral M. Studies on mechanical behaviour and tensile fractography of boron carbide particles reinforced Al8081 alloy advanced metal composites. Materials Today: Proceedings.2022; 52: 2115–2120. https: //d oi. org/ 10. 10 16 / j.matpr.2021.12.397
27. Nagaral M., Auradi V., Bharath B. Mechanical characterization and fractography of 100 micron sized silicon carbide particles reinforced Al6061 alloy composites. Metallurgical and Materials Engineering.2022; 28(1): 17–32. https://doi.org/10.30544/639
28. Angadi S., Kumar S., Nagaral M., Auardi V., Valukula B. Effect of ceramic boron carbide particles addition on the mechanical and microstructural characteristics of Al7020 alloy composites. Mechanics of advanced composite structures. 2025; 12(24): 169–180. https :// d o i 1 0.22075/macs.2024.33857.1655
29. Madeva N. Vijaykumar H. Virupaxi A. Satish K. Influence of two-stage stir casting process on mechanical characterization and wear behavior of AA2014-ZrO_2 nano-composites. Transactions of the Indian Institute of Metals. 2018; 71(5): 2845–2850. https:// 10.1007/s12666-018-1441-6
30. Chebolu R., Nallu R., Chanamala R., Kumar S., Rudrapati R. Influence of SiC/TiB_2 particles addition on corrosion behavior of As-Cast Zn-Al-Cu Alloy hybrid composites. Hindawi Journal of Engineering. 2022; 3(4): 1–5. https://doi.org/10.1155/2022/3669584
31. B.Hussein, M.Iman, J. Abdul. Mechanical properties and wear behaviour of Al 6061 matrix composites with hybrid reinforcements through powder metallurgy technique. Diyala Journal of Engineering Sciences. 2025; 18(2): 191–202191. https: //doi.org/1 0.2423 7/djes.2024.18212
32. Gaitonde V., Karnik S., Jayaprakash M.Some studies on wear and corrosion properties of Al5083\Al2O3\G hybrid composites. Journal of minerals and materials characterization and engineering.2012; 11(7): 695–703. https:// doi: 10.4236/jmmce.2012.117055
33. Fontana M.G. Corrosion Engineering. McGraw-Hill, 1987.
34. Jones D.A. Principles and Prevention of Corrosion. Prentice Hall, 1996.
35. Singh J., Chauhan A., Sharma V. Corrosion behaviour of aluminium metal matrix composites: A review. Materials Today Proceedings. 1987; 18: 5524–5531. https: // d o i. o rg /10.1016/j.matpr.2015.07.29